J Neurophysiol 97: 540–549, 2007.
First published November 1, 2006; doi:10.1152/jn.00905.2006.

Nerve-Evoked Synchronous Release and High K^+-Induced Quantal Events Are Regulated Separately by Synaptotagmin I at *Drosophila* Neuromuscular Junctions

Takuya Tamura, Jiamei Hou, Noreen E. Reist, and Yoshiaki Kidokoro
Institute for Molecular and Cellular Regulation, Gunma University, Maebashi, Japan

Submitted 24 August 2006; accepted in final form 29 October 2006

Tamura T, Hou J, Reist NE, Kidokoro Y. Nerve-evoked synchronous release and high K^+-induced quantal events are regulated separately by synaptotagmin I at *Drosophila* neuromuscular junctions. *J Neurophysiol* 97: 540–549, 2007. First published November 1, 2006; doi:10.1152/jn.00905.2006. The distal Ca^{2+}-binding domain of synaptotagmin I (Syt I), C2B, has two Ca^{2+}-binding sites. To study their function in *Drosophila*, pairs of aspartates were mutated to asparagines and the mutated *syt I* was expressed in the *syt I*–null background ($P[syt\ I^{B\text{-}D1,2N}]$ and $P[syt\ I^{B\text{-}D3,4N}]$). We examined the effects of these mutations on nerve-evoked synchronous synaptic transmission and high K^+-induced quantal events at embryonic neuromuscular junctions. The $P[syt\ I^{B\text{-}D1,2N}]$ mutation virtually abolished synaptic transmission, whereas the $P[syt\ I^{B\text{-}D3,4N}]$ mutation strongly reduced but did not abolish it. The quantal content in $P[syt\ I^{B\text{-}D3,4N}]$ increased with the external Ca^{2+} concentration, $[Ca^{2+}]_e$, with a slope of 1.86 in double-logarithmic plot, whereas that of control was 2.88. In high K^+ solutions the quantal event frequency in $P[syt\ I^{B\text{-}D3,4N}]$ increased progressively with $[Ca^{2+}]_e$ between 0 and 0.15 mM as in control. In contrast, in $P[syt\ I^{B\text{-}D1,2N}]$ the event frequency did not increase progressively between 0 and 0.15 mM and was significantly lower at 0.15 than at 0.05 mM $[Ca^{2+}]_e$. The $P[syt\ I^{B\text{-}D1,2N}]$ mutation inhibits high K^+-induced quantal release in a narrow range of $[Ca^{2+}]_e$ (negative regulatory function). When Sr^{2+} substituted for Ca^{2+}, nerve-evoked synchronous synaptic transmission was severely depressed and delayed asynchronous release was appreciably increased in control embryos. In high K^+ solutions with Sr^{2+}, the quantal event frequency was higher than that in Ca^{2+} and increased progressively with $[Sr^{2+}]_e$ in control and in both mutants. Sr^{2+} partially substitutes for Ca^{2+} in synchronous release but does not support the negative regulatory function of Syt I.

INTRODUCTION

Synaptotagmin I (Syt I) has two Ca^{2+}-binding domains, C2A and C2B, and is considered to be a major Ca^{2+} sensor for nerve-evoked synchronous synaptic transmission (Kidokoro 2003; Koh and Bellen 2003; Südhof and Rizo 1996). Recent findings support the idea that Ca^{2+} binding to the C2B domain is essential for such synaptic transmission (Mackler et al. 2002; Nishiki and Augustine 2004b; Robinson et al. 2002). In addition, Mackler et al. (2002) generated two strains of transformants in each of which two negatively charged aspartates (D) that coordinate the binding of Ca^{2+} were mutated to asparagines (N). The mutated *syt I* was expressed in the *syt I*–null background and synaptic transmission was examined at the neuromuscular junction (NMJ). One transformant, $P[syt\ I^{B\text{-}D3,4N}]$, survived beyond third instars. The mean amplitude of nerve-evoked synchronous synaptic potentials in $P[syt\ I^{B\text{-}D3,4N}]$ was reduced to <1% of the control in which wild-type *syt I* was expressed in the *syt I*–null background ($P[syt\ I^{WT}]$). The other transformant, $P[syt\ I^{B\text{-}D1,2N}]$, did not survive beyond the embryonic stage and synaptic transmission was studied in third instar larvae expressing $syt\ I^{WT}$ and $P[syt\ I^{B\text{-}D1,2N}]$. The mean amplitude of nerve-evoked synchronous synaptic potentials was reduced to <10% of control (Mackler et al. 2002).

In cultured mouse hippocampal neurons, Nishiki and Augustine (2004b) examined the mutations of each of aspartate (D) to asparagine (N) in the C2B domain on nerve-evoked synaptic transmission. When they expressed mutated Syt I(D2N) (D at position 309) or Syt I(D3N) (D at position 363) in *syt I* knockout synapses, synchronous synaptic currents were virtually abolished, whereas asynchronous release was not enhanced as in *syt I* knockout synapses. On the other hand, the substitution of D to N at positions 303 (D1), 365 (D4), and 371 (D5) had relatively minor effects on synaptic transmission. They concluded that Ca^{2+}-binding sites in C2B are essential for fast synaptic transmission. Furthermore, because in *syt I*(*D2N*) and *syt I*(*D3N*), delayed asynchronous release was not enhanced as in *syt I* knockout synapses, they concluded that Syt I has dual functions: synchronization of fast release and suppression of delayed release.

We sought to address the dual roles of Syt I in synaptic transmission using *Drosophila syt I* mutants. The previous study (Mackler et al. 2002) was limited in three aspects; *1*) Synaptic transmission in $P[syt\ I^{B\text{-}D1,2N}]$ lines could not be studied in the *syt I*–null background because the mutant did not survive beyond the embryonic stage. *2*) In $P[syt\ I^{B\text{-}D3,4N}]$ third instars, synaptic transmission at the NMJ might have been modified during development as the result of defective synaptic transmission and may not quantitatively reflect the effect of mutation per se. *3*) Synaptic transmission was assessed as membrane potential changes, thus impairing quantitative comparisons with previous results from voltage-clamp experiments. To cover these shortfalls, in this study we examined synaptic transmission in $P[syt\ I^{B\text{-}D3,4N}]$ and $P[syt\ I^{B\text{-}D1,2N}]$ embryos in the absence of wild-type *syt I* using patch-clamp techniques and found that synaptic transmission at NMJs was severely reduced in the former and virtually abolished in the latter. We concluded that both Ca^{2+}-binding sites in the C2B domain are essential for synchronous synaptic transmission. We then examined the negative regulatory function of Syt I on high K^+-induced vesicle fusion in these transformants and found in $P[syt\ I^{B\text{-}D1,2N}]$ that the frequency of high K^+-induced

Address for reprint requests and other correspondence: Y. Kidokoro, Department of Physiology, David Geffen School of Medicine at UCLA, 10833 Le Conte Avenue, Los Angeles, CA 90095-1751 (E-mail; ykidokoro@mednet.ucla.edu).

The costs of publication of this article were defrayed in part by the payment of page charges. The article must therefore be hereby marked "*advertisement*" in accordance with 18 U.S.C. Section 1734 solely to indicate this fact.

quantal events was Ca^{2+}-dependently depressed. In addition, by substituting Sr^{2+} for Ca^{2+} we found that Sr^{2+} partially substitutes for Ca^{2+} in synchronous release but does not support the negative regulatory function of Syt I. Thus the negative regulatory function is unique to Ca^{2+}.

METHODS

Fly strains

There are five aspartate residues forming two Ca^{2+}-binding sites in the C2B domain of Syt I (Fernandez et al. 2001). The following transformants that have amino acid substitutions in those residues were used in this study (Mackler et al. 2002). In one transformant the third and fourth aspartate residues were mutated to asparagines (D416,418N), and the mutant transgene was expressed in the *syt I*–null background (*syt* I^{AD4}; DiAntonio and Schwarz 1994). This line is referred to as *P*[*syt* $I^{B\text{-}D3,4N}$]. In the second transformant the first and second aspartate residues were mutated to asparagines (D356,362N) and expressed in the *syt I*–null background. This line is referred to as *P*[*syt* $I^{B\text{-}D1,2N}$]. As a control, wild-type *syt I* was expressed in the *syt I*–null background (referred to as *P*[*syt* I^{WT}]). Genotypes of the transgenic lines used were: *P*[*syt* I^{wt}] = *yw; syt* I^{AD4}/*syt* I^{AD4}*P*[*elav Gal4*]; *P*[*UAS syt* I^{wt}]/+, *P*[*syt* $I^{B\text{-}D3,4N}$] = *yw; syt* I^{AD4}/*syt* I^{AD4}*P*[*elav Gal4*]; *P*[*UAS syt* $I^{B\text{-}D3,4N}$]/+, and *P*[*syt* $I^{B\text{-}D1,2N}$] = *yw; syt* I^{AD4}/*syt* I^{AD4}*P*[*elav Gal4*]; *P* [*UAS syt I* $^{B\text{-}D1,2N}$]/+.

Solutions

The ionic composition of Ca^{2+}-free saline used for dissection of embryos was (in mM): NaCl, 140; KCl, 2; $MgCl_2$, 6; and HEPES-NaOH, 5 (pH 7.1). For nerve stimulation to evoke synaptic currents and for experiments with Ca^{2+} ionophores, HL3 solution was used and the Ca^{2+} concentration was changed by substituting the same amount of Mg^{2+}. The ionic composition of HL3 solution was as follows (in mM): NaCl, 70; KCl, 5; $CaCl_2$, 1.5; $MgCl_2$, 20; $NaHCO_3$, 10; Trehalose, 5; sucrose, 115; and HEPES-NaOH, 5 (pH, 7.1) (Stewart et al. 1994). The ionic composition of high K^+ solution was (in mM): NaCl, 80; KCl, 62; $MgCl_2$, 6; and HEPES-NaOH, 5 (pH, 7.1). To study the effect of Ca^{2+}, $CaCl_2$ (0.05–0.20 mM) was added by replacing the same amount of $MgCl_2$. In high K^+ solutions the Mg^{2+} concentration was kept relatively high compared with changes in [Ca^{2+}] so that the effect on surface negative charges of the presynaptic membrane was minimal (Hagiwara and Takahashi 1967). The Ca^{2+} concentration in the nominally zero Ca^{2+} high K^+ solution was about 0.6 μM, which should not affect our conclusions. The internal solution for the patch pipette had the following ionic composition (in mM): CsCl, 158; EGTA, 5; HEPES-NaOH, 10; and ATP, 2 (pH 7.1).

Preparations and recording conditions

Embryos (19–21 h after fertilization) of transformants and controls were used in this study. Dissecting procedures were the same as described previously (Kidokoro and Nishikawa 1994; Nishikawa and Kidokoro 1995) and carried out in Ca^{2+}-free saline. After treating the dissected preparation with collagenase (1 mg/ml) for 30 s to 2 min, synaptic currents were recorded with patch-clamp techniques in the whole cell configuration from abdominal longitudinal muscle #6. The series resistance of the recording electrode, which varied between 5 and 30 MΩ, was compensated at an 80% level. The membrane potential was held at -60 mV. The internal solution contained Cs^+ and the junction potential of electrodes filled with the Cs^+ internal solution was -5 mV in normal saline (HL3 solution). Thus the true holding potential was -65 mV.

Nerve stimulation and calculation of the quantal content

For nerve stimulation, the tip of a microelectrode, which has a resistance of 10 to 20 MΩ after being filled with 4 M K-acetate, was placed in the ventral nerve cord near the exit of the segmental nerve, and rectangular pulses of 1-ms duration and about 2-μA intensity were delivered at 0.3 Hz. In the case of *syt I* mutants, each stimulus did not necessarily produce a synaptic current, which made it difficult to judge whether the stimulation was effective. However, even in those cases, tetanic stimulation (10 Hz for 2 s) invariably increased asynchronous release, thus indicating its effectiveness. Then the stimulus frequency was switched to 0.3 Hz to collect data. To determine the quantal content, we used the failure method assuming the Poisson process for synaptic transmission (Katz 1969), that is, the quantal content: $m = -\ln (n_0/N)$, where ln is the natural logarithm, n_0 is the number of failures, and N is the total number of stimuli. We adopted this method because in developing synapses the amplitudes of minis were not normally distributed and varied widely (Zhang et al. 1999). Thus it is not certain whether the mean amplitude of minis is equal to the quantal size.

Hypertonicity and Ca^{2+} ionophore responses

A hypertonic solution was prepared by adding 420 mM sucrose to the Ca^{2+}-free external solution. A Ca^{2+} ionophore, A23187 (20 μM), was dissolved in HL3 solution containing 0.5 mM Ca^{2+}. These solutions were applied to the NMJ by the puff method with a gas pressure of 0.5 kg/cm^2 for 11 s. The puff pipette had a tip diameter of 3–5 μm and the tip was placed within about 20 μm of the junctional area. The quantal synaptic events were counted individually every 0.5 s. The total number of events during each response was counted during a period of 30 s starting at the onset of puff pulse. For application of A23187 the bath solution was the Ca^{2+}-free HL3 solution containing 20 μM A23187.

All experiments were carried out at room temperature (18–27°C).

CHEMICALS. Tetrodotoxin (TTX) and collagenase were purchased from Sigma (St. Louis, MO). A23187 was obtained from Alomone Labs (Jerusalem, Israel). A23187 was dissolved in DMSO at 5 mM and stock solutions were stored at -20°C.

STATISTICAL ANALYSES. For comparison among multiple groups, ANOVA was used with the Tukey test. For comparison of two groups, Student's *t*-test was used.

RESULTS

To study the role of Ca^{2+}-binding sites in the C2B domain for synchronous synaptic transmission and the negative regulatory function of Syt I on asynchronous release at the neuromuscular junction (NMJ) in embryos, we used two transformants. In one transformant, two aspartate residues in positions 356 (D1) and 362 (D2) were mutated to asparagines (N) and expressed in the *syt I*–null background (*syt* I^{AD4}; DiAntonio and Schwarz 1994). This transformant is referred to as *P*[*syt* $I^{B\text{-}D1,2N}$]. In the other transformant, two aspartates in position 416 (D3) and 418 (D4) were mutated to asparagines and expressed in the *syt I*–null background, which is referred to as *P*[*syt* $I^{B\text{-}D3,4N}$]. As a control, we used a strain in which wild-type *syt I* is expressed in the *syt I*–null background, which is referred to as *P*[*syt* I^{WT}] (Mackler et al. 2002).

Nerve-evoked synchronous synaptic transmission at the NMJ in syt I transformant embryos

The nerve was stimulated at 0.3 Hz with a microelectrode, the tip of which was placed in the CNS at the corresponding

segment and nerve-evoked synaptic currents were recorded as described previously (Deitcher et al. 1998). In control embryos, *P*[*syt I*^{WT}], bathed in HL3 containing 1 mM Ca^{2+}, the majority of nerve stimulations produced synaptic currents (Fig. 1*A2*). The synaptic events occurred predominantly between 2 and 10 ms after the onset of the stimulation pulse as shown in the event frequency histogram in Fig. 1*A1* (99 events in the first bin, between 2 and 10 ms, responding to 102 stimuli). Some cells also exhibited delayed synaptic events (three of eight cells examined at 1 mM Ca^{2+}). The average of entries in eight bins after stimulation (excluding the first bin) was 0.88 ± 1.13 (mean ± SD; data in the text are expressed in this format hereafter, unless otherwise stated.). Some of the spontaneous and delayed quantal events may occur during the first bin. To correct for a contribution of these events in the first bin, we subtracted the average number of entry of the following eight bins (0.88/bin) from the entry number in the first bin (99) to estimate the number of events synchronous to nerve stimulation (98.1). (This correction procedure is based on the assumption that the mechanism underlying the delayed release is also operating during the period covered by the first bin; Goda and Stevens 1994.) The quantal content was calculated by the failure method assuming Poisson statistics (Katz 1969). Accordingly, the quantal content of the *P*[*syt I*^{WT}] cell shown in Fig. 1*A* is 1.75 (=−ln[(102 − 98.1)/102]). The mean quantal content of *P*[*syt I*^{WT}] embryos at 1 mM Ca^{2+} was 1.65 ± 0.47 (mean ± SD, $n = 8$). The quantal content in this transgenic control line was smaller than that in the control line where wild-type *syt I* was expressed from the native *syt I* gene used in a previous study under the same experimental condition (2.5 ± 0.6; Okamoto et al. 2005). This finding is in accord with the report by Mackler and Reist (2001) that a significantly smaller mean evoked synaptic potential (67% of the native wild-type control) was observed in third instar *P*[*syt I*^{WT}] larvae.

In *P*[*syt I*$^{B\text{-}D3,4N}$] embryos, synchronous synaptic transmission at the NMJ was dramatically reduced but not abolished (Fig. 1, *B1* and *B2*). The majority of stimuli did not evoke synaptic currents during a window between 2 and 10 ms after the onset of the stimulation pulse in 2 mM Ca^{2+} (Fig. 1*B1*; note that the scale in the ordinate is much smaller here compared with that in *A1*). However, some quantal events did occur with appropriate timing and the number of entries in the first bin between 2 and 10 ms was significantly larger than the

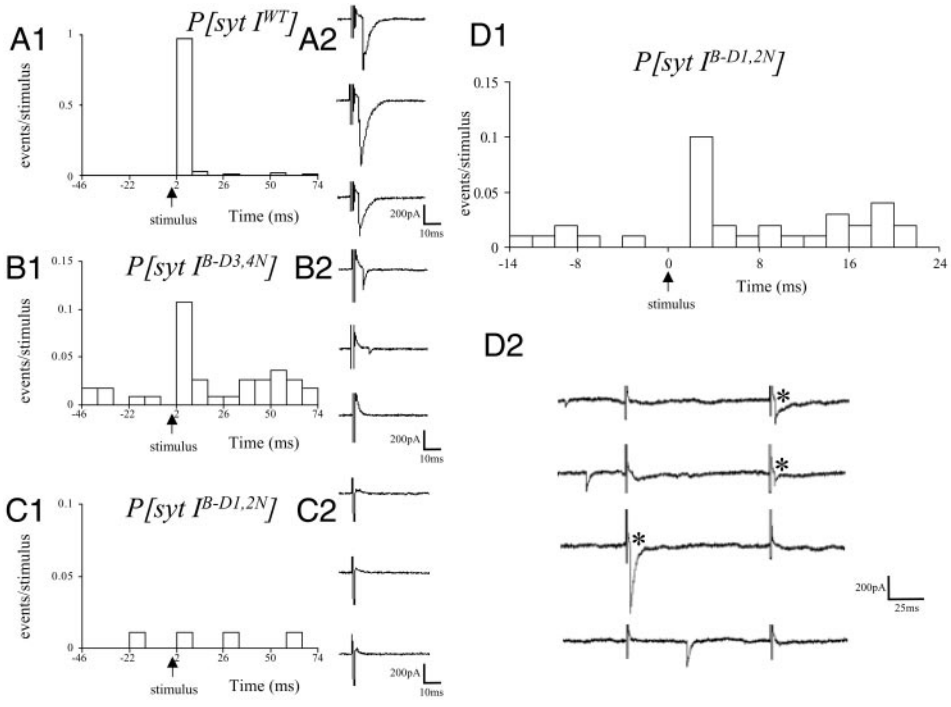

FIG. 1. Nerve-evoked synchronous and asynchronous synaptic currents in a wild-type (*A*) and two *syt I* transformants (*B*, *C*, and *D*). *A1* and *A2*: a frequency histogram (*A1*) and sample traces (*A2*) of synaptic events evoked by nerve stimulation obtained in a muscle cell of a *P*[*syt I*^{WT}] embryo. Synchronous synaptic events are seen in the first bin after stimulation (during a period between 2 and 10 ms after the onset of the stimulus pulse). Some asynchronous synaptic events were observed that are depicted in the bins 10 ms or later after stimulation. Events preceding the stimulus are spontaneously occurring events. Total number of stimuli was 102. Sample current traces are shown in *A2*. Recordings were carried out in HL3 medium containing 1.0 mM Ca^{2+} and 20.5 mM Mg^{2+}. Holding potential was −65 mV; stimulus frequency was 0.3 Hz. Data obtained in this experimental condition in various external Ca^{2+} concentrations ($[Ca^{2+}]_e$) are plotted in Fig. 3. *B1* and *B2*: a frequency histogram (*B1*) and sample traces (*B2*) of synaptic events evoked by nerve stimulation obtained in a muscle cell of a *P*[*syt I*$^{B\text{-}D3,4N}$] embryo. Synchronous synaptic events are seen in the first bin after stimulation (during a period between 2 and 10 ms). Some asynchronous synaptic events were observed and are depicted in the bins 10 ms or later after stimulation. Total number of stimuli was 112. Sample current traces are shown in *B2*. Recordings were carried out in HL3 medium containing 2 mM Ca^{2+} and 19.5 mM Mg^{2+}. Holding potential was −65 mV; stimulus frequency was 0.3 Hz. Data obtained in this experimental condition in various $[Ca^{2+}]_e$ are plotted in Fig. 3. *C1* and *C2*: a frequency histogram (*C1*) and sample traces (*C2*) of synaptic events evoked by nerve stimulation obtained in a muscle cell of a *P*[*syt I*$^{B\text{-}D1,2N}$] embryo. No nerve-evoked synaptic events were observed. Total number of stimuli was 94. Sample current traces are shown in *C2*. Recordings were carried out in HL3 medium containing 5 mM Ca^{2+} and 16.5 mM Mg^{2+}. Stimulus frequency was 0.3 Hz. *D1* and *D2*: a frequency histogram (*D1*) and sample traces (*D2*) of synaptic events evoked by nerve stimulation obtained in a muscle cell of a *P*[*syt I*$^{B\text{-}D1,2N}$] embryo. Synchronous synaptic events are seen in the first bin after stimulation (during a period between 2 and 4 ms). Total number of stimuli was 112. Sample current traces are shown in *D2*. Synchronous events are indicated by asterisks. Recordings were carried out in HL3 medium containing 5 mM Ca^{2+} and 16.5 mM Mg^{2+}. Stimulus frequency was 10 Hz.

mean entry in other bins. After delivery of 112 stimuli at 0.3 Hz the number of entries in the first bin was 12 and the average entry in the following eight bins was 2.5 ± 1.1 events/bin. After correcting the entry in the first bin for a contribution of delayed and spontaneous events, the failure rate was calculated to be 0.92 and the quantal content to be 0.08 (= −ln 0.92). The average quantal content of six cells was 0.097 ± 0.041.

In contrast, *P*[*syt I*$^{B\text{-}D1,2N}$] embryos exhibited neither synchronous synaptic transmission nor delayed asynchronous release when stimulated at 0.3 Hz in 5 mM Ca^{2+} ($n = 6$). Figure 1, *C1* and *C2* shows this lack of response observed in one cell after delivery of 94 stimuli. Furthermore, these negative results were confirmed in eight cells in 1.5 mM external Ca^{2+} concentration ($[Ca^{2+}]_e$) (data not shown). This total lack of synaptic transmission in *P*[*syt I*$^{B\text{-}D1,2N}$] is in contrast to rare but significant synchronous synaptic transmission in *syt I*^{null} embryos (Broadie et al. 1994; Kidokoro 2003; Okamoto et al. 2005). Thus the presence of mutated Syt I in *P*[*syt I*$^{B\text{-}D1,2N}$] suppresses the function of another Ca^{2+} sensor (a second, non-Syt I, Ca^{2+} sensor) for synchronous synaptic transmission that operates in the absence of Syt I.

The mutated Syt I in *P*[*syt I*$^{B\text{-}D1,2N}$] also depresses the function of wild-type Syt I for synchronous synaptic transmission because in heterozygous third instar larvae expressing both *syt I*^{WT} and *P*[*syt I*$^{B\text{-}D1,2N}$], nerve-evoked synchronous synaptic potentials were reduced to <10% of control, whereas in larvae expressing wild-type *syt I* and *P*[*syt I*$^{B\text{-}D3,4N}$] the mean amplitude of synaptic potentials was reduced to roughly 50% of the control (Mackler et al. 2002).

However, in one single cell (out of five examined) when the nerve was stimulated at 10 Hz in 5 mM Ca^{2+}, a very few evoked quantal synaptic events with appropriate timing occurred (Fig. 1, *D1* and *D2*, marked with asterisks). This finding indicates that synchronous synaptic transmission in *P*[*syt I*$^{B\text{-}D1,2N}$] can be evoked, although extremely rarely. This finding suggests that Ca^{2+} binds to the mutated Syt I in *P*[*syt I*$^{B\text{-}D1,2N}$] and facilitates vesicle fusion.

Responses to a Ca^{2+} ionophore in P[syt I$^{B\text{-}D1,2N}$] embryos

So far we found that in *P*[*syt I*$^{B\text{-}D1,2N}$] synchronous transmitter release to nerve stimulation was virtually abolished and attributed this defect to a disability of mutated Syt I to sense Ca^{2+}. However, Syt I interacts with presynaptic Ca^{2+} channels by the synprint motif of the channel (Catterall 1999). It is then possible that the observed defect in synaptic transmission arises from a lack of Ca^{2+} influx during depolarization in this transformant. Although this motif in the Ca^{2+} channel is missing in *Drosophila* (Littleton and Ganetzky 2000), it is still possible that another motif substitutes for it in this animal.

To test this possibility we bypassed voltage-gated Ca^{2+} channels with a Ca^{2+} ionophore and directly measured the Ca^{2+} sensitivity of the vesicle fusion machinery in *P*[*syt I*$^{B\text{-}D1,2N}$] embryos. As shown in Fig. 2, the response to puff-applied ionophore (20 μM A23187 with 0.5 mM Ca^{2+}) in *P*[*syt I*$^{B\text{-}D1,2N}$] was reduced to roughly 16% of the control in the peak frequency. Thus the Ca^{2+} sensitivity of the Ca^{2+} sensor for vesicle fusion was dramatically reduced in this transformant, but the elevation of Ca^{2+} level was detected, although poorly. Because similar residual responses, 9–14% of the control, to Ca^{2+} ionophores were observed even in *syt I*^{AD4}, a *syt I*–null allele (Okamoto et al. 2005), the increased Ca^{2+} level may be detected in *P*[*syt I*$^{B\text{-}D1,2N}$] by either the mutated Syt I or the second Ca^{2+} sensor.

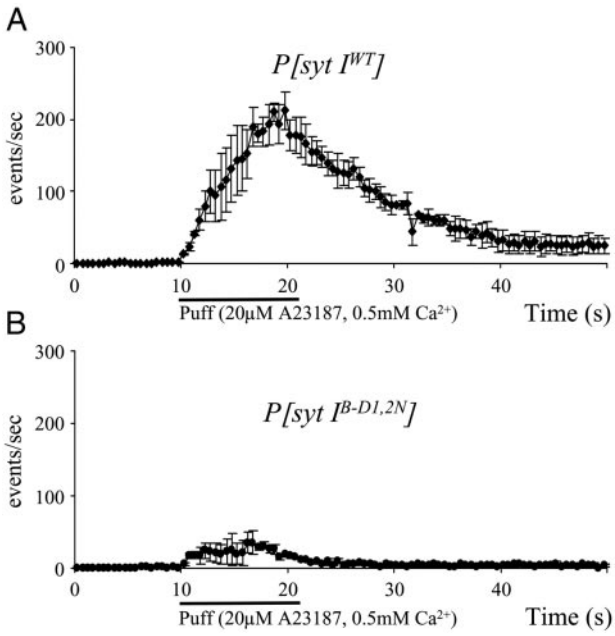

FIG. 2. Effect of Ca^{2+} ionophores on quantal release of transmitter in *P*[*syt I*^{WT}] (*A*) and in *P*[*syt I*$^{B\text{-}D1,2N}$] (*B*). *A*: number of events per second is plotted against time. HL3 solution containing 20 μM A23187 and 0.5 mM Ca^{2+} was puff-applied for 11 s to *P*[*syt I*^{WT}] embryos. Timing of the puff is indicated by a horizontal bar below the abscissa. Bath was filled with Ca^{2+}-free HL3 solution containing 20 μM A23187. Vertical bars attached to each point are the SE ($n = 3$). *B*: same as *A*. HL3 solution containing 20 μM A23187 and 0.5 mM Ca^{2+} was applied to *P*[*syt I*$^{B\text{-}D1,2N}$] embryos ($n = 6$).

Ca^{2+} dependency of nerve-evoked synchronous synaptic transmission in P[syt I$^{B\text{-}D3,4N}$] embryos

Next we examined the external Ca^{2+} dependency of synchronous synaptic currents in *P*[*syt I*$^{B\text{-}D3,4N}$] embryos. The quantal content increased with external Ca^{2+} between 1 and 5 mM, and a straight line was fitted to these points on a double-logarithmic plot using the least-squares method (Fig. 3). At 1 mM $[Ca^{2+}]_e$ the quantal content in *P*[*syt I*$^{B\text{-}D3,4N}$] embryos was 1/100 of that in *P*[*syt I*^{WT}]. The slope *N* was 1.86 ± 0.40 (mean ± SE of estimate, $n = 32$), which is significantly smaller than that in the control (2.88 ± 0.43, $n = 34$, $P < 0.05$). The value for *N* in *P*[*syt I*^{WT}] is not different from that in control embryos with wild-type *syt I* (3.01 ± 0.36; Okamoto et al. 2005). Thus the *P*[*syt I*$^{B\text{-}D3,4N}$] mutation reduced the value of *N*, suggesting that the Ca^{2+}-binding sites in the C2B domain sense Ca^{2+} for synchronous synaptic transmission. It should be noted that the apparent cooperativity *N* for *P*[*syt I*$^{B\text{-}D3,4N}$] is significantly larger than that for *syt I*^{null} (0.95 ± 0.36, $P < 0.05$; Okamoto et al. 2005), indicating that the mutated Syt I in *P*[*syt I*$^{B\text{-}D3,4N}$] is sensing Ca^{2+} for synchronized synaptic transmission. [The data presented in this study were obtained under identical experimental conditions during the period mostly overlapping as those described in Okamoto et al. (2005). Thus a direct comparison of the data should be meaningful.]

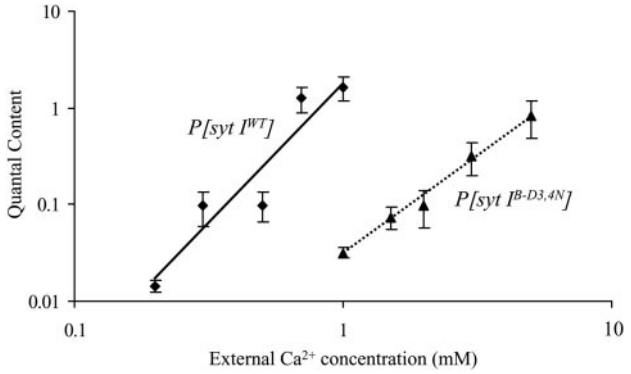

FIG. 3. Relationship between the quantal content and $[Ca^{2+}]_e$ in the double-logarithmic plot in *P*[*syt* I^{WT}] (diamonds) and *P*[*syt* $I^{B\text{-}D3,4N}$] (triangles) mutant embryos. All data depicted in this figure were obtained in the experimental condition described in Fig. 1. Quantal content was estimated by the failure method assuming the Poisson distribution of evoked events (Katz 1969). Quantal content, $m = -\ln(n_0/N)$, where n_0 is the number of failures and N is the total number of stimuli. Vertical bars attached to each point are the SE. Straight line was fitted to all the data points (not means) by the least-squares method. Number of cells examined was between 4 and 6 for each Ca^{2+} concentration.

Miniature synaptic currents in P[syt $I^{B\text{-}D1,2N}$] and P[syt $I^{B\text{-}D3,4N}$] embryos

In the HL3 solution containing 1.5 mM Ca^{2+} and 3 μM TTX, spontaneous synaptic currents (miniature synaptic currents, or minis) occurred infrequently. The mean frequencies were 1.2 ± 1.0/min ($n = 9$) and 2.0 ± 2.0/min ($n = 10$) in *P*[*syt* $I^{B\text{-}D1,2N}$] and *P*[*syt* $I^{B\text{-}D3,4N}$], respectively. These values are not significantly different from those in *P*[*syt* I^{WT}], 2.6 ± 2.9/min ($n = 15$; $P > 0.05$). This finding indicates that the negative regulatory function of Syt I is operating in these transformants. In contrast, Mackler et al. (2002) reported that the mini frequency in *P*[*syt* $I^{B\text{-}D3,4N}$] third instar larvae was twofold higher than that in *P*[*syt* I^{WT}]. This might be the result of developmental modification of NMJs during the period from embryos to third instar larvae in this transformant.

$[Ca^{2+}]_e$ dependency of the frequency of high K^+-induced quantal synaptic events

In high K^+ solutions, the presynaptic terminal membrane is continuously depolarized and voltage-gated Ca^{2+} channels open asynchronously, unlike the synchronized opening induced by nerve stimulation. In this situation the elevated cytosolic Ca^{2+} in the terminal is most likely to be detected by a high-affinity, second Ca^{2+} sensor that has been postulated to explain delayed asynchronous release after nerve stimulation (Geppert et al. 1994; Goda and Stevens 1994). We assume, for the sake of simplicity, that synchronous as well as asynchronous release observed in *syt* I^{null} mutants is mediated by this second Ca^{2+} sensor (Okamoto et al. 2005). Nevertheless, Syt I is also involved in regulation of these quantal synaptic events because mutations in *syt I* profoundly affect the frequency of high K^+-induced synaptic events (Okamoto et al. 2005; this study).

Synaptic events were induced in high K^+ solutions (62 mM K^+ and 3 μM TTX) containing Ca^{2+} between 0 and 0.20 mM in the control, *P*[*syt* I^{WT}], and the two *syt I* transformants. In *P*[*syt* I^{WT}], the frequency of high K^+-induced quantal events was low in 0 mM $[Ca^{2+}]_e$ but increased progressively ≤0.15 mM and abruptly at 0.20 mM (Fig. 4*A*, diamonds). In *P*[*syt* $I^{B\text{-}D3,4N}$] embryos a similar dependency of the quantal event frequency was observed as $[Ca^{2+}]_e$ was increased (Fig. 4*A*, triangles). In contrast, in *P*[*syt* $I^{B\text{-}D1,2N}$] embryos, the frequency was not different from that in the control at 0 and 0.05 mMCa^{2+} but significantly lower at 0.10 and 0.15 mM than those in the control ($P < 0.05$) (Fig. 4*A*, circles). Furthermore, the frequency in *P*[*syt* $I^{B\text{-}D1,2N}$] at 0.15 mM was significantly lower than that at 0.05 mM $[Ca^{2+}]_e$ (Fig. 4*B*), but increased abruptly at 0.20 mM (Fig. 4*A*, circle). These results indicate that in the Ca^{2+} range around 0.15 mM the mutated Syt I in *P*[*syt* $I^{B\text{-}D1,2N}$] is inhibiting high K^+-induced vesicle fusion in a Ca^{2+}-dependent manner.

In *P*[*syt* $I^{B\text{-}D1,2N}$] the frequency of quantal events increased from nominal zero to 0.05 mM $[Ca^{2+}]_e$ and between 0.15 and 0.20 mM. The value at 0.05 mM [43.8 ± 27.3/min ($n = 9$)] is

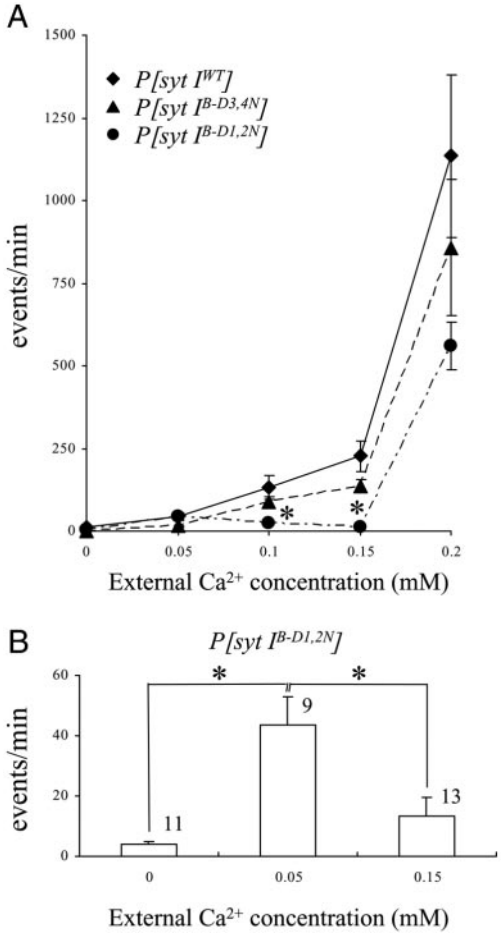

FIG. 4. Relationship between the frequency of quantal synaptic events induced by high K^+ and the external Ca^{2+} concentration. *A*: quantal events were recorded in the external solution containing 62 mM K^+, 3 μM tetrodotoxin (TTX), and various Ca^{2+} concentrations in embryos of *P*[*syt* I^{WT}] (diamonds), *P*[*syt* $I^{B\text{-}D3,4N}$] (triangles), and *P*[*syt* $I^{B\text{-}D1,2N}$] (circles). Quantal events were counted during a period between 0.5 and 10 min of recording depending on the frequency. Vertical bars attached to each point are the SE. Number of cells for each point was between 4 and 12. Event frequency was measured in several cells at a given concentration of Ca^{2+} and the experiment was repeated in various Ca^{2+} concentrations. *B*: same data plotted in *A* for *P*[*syt* $I^{B\text{-}D1,2N}$] are replotted to demonstrate a Ca^{2+}-dependent decrease of event frequency. Asterisks indicate statistical differences at $P = 0.05$. Numbers attached to each column are the number of cells examined.

higher than that in *syt* I^{AD4} (11.7 ± 11.2/min, $n = 13$, $P < 0.01$; Okamoto et al. 2005). This finding suggests that mutated Syt I in *P*[*syt* $I^{B\text{-}D1,2N}$] binds Ca^{2+} and facilitates vesicle fusion.

Hypertonicity responses in P[syt $I^{B\text{-}D1,2N}$] and P[syt $I^{B\text{-}D3,4N}$] embryos

The lower frequencies of high K^+-induced quantal events in *P*[*syt* $I^{B\text{-}D1,2N}$] compared with those in *P*[*syt* I^{WT}] could be a result of fewer release-ready synaptic vesicles at the NMJ. To assess the population of release-ready vesicles, we next examined the hypertonicity response. The quantal event frequency increases with puff application of hypertonic solutions at embryonic NMJs (Suzuki et al. 2002a). Because Ca^{2+} is not required for this response (Rosenmund and Stevens 1996), the population of release-ready vesicles can be assessed regardless of Ca^{2+} sensitivity of the release mechanism.

The hypertonicity response evoked with 420 mM sucrose added to Ca^{2+}-free HL3 in *P*[*syt* I^{WT}] (Fig. 5*A*; total number of events, 291 ± 40, Fig. 5*D*, *left column*; peak frequency, 66 ± 20/s, $n = 5$, Fig. 5*E*, *left column*) was not different from that previously reported for wild-type embryos (Okamoto et al. 2005; Suzuki et al. 2002a,b). Furthermore, the response in *P*[*syt* $I^{B\text{-}D3,4N}$] (Fig. 5*B*; total number of events, 286 ± 35; Fig. 5*D*, *right column*; peak frequency, 73 ± 21/s, $n = 5$, Fig. 5*E*, *right column*) was not different from that in *P*[*syt* I^{WT}]. This finding is in accord with the findings in the third instars where neither the hypertonicity response (Mackler et al. 2002) nor the abundance of synaptic vesicles (Loewen et al. 2006) was disrupted in *P*[*syt* $I^{B\text{-}D3,4N}$] larvae. However, the hypertonicity response in *P*[*syt* $I^{B\text{-}D1,2N}$] embryos (Fig. 5*C*) was significantly smaller than that in *P*[*syt* I^{WT}] (total number of events, 201 ± 57, Fig. 5*D*, *middle column*; peak frequency, 45 ± 10/s, $n = 6$, Fig. 5*E*, *middle column*). This smaller response (roughly 70% of controls), however, does not explain the severe defect in nerve-evoked synchronous synaptic transmission (Fig. 1) nor the lower frequency of high K^+-induced quantal events in *P*[*syt* $I^{B\text{-}D1,2N}$] at 0.1 and 0.15 mM [Ca^{2+}] (Fig. 4).

The hypertonicity response in *syt* I^{AD4} is reduced further than that in *P*[*syt* $I^{B\text{-}D1,2N}$] (nearly 10% of controls), yet the defect in synchronous release is less severe (Okamoto et al. 2005), suggesting that the mutated Syt I in *P*[*syt* $I^{B\text{-}D1,2N}$] predominantly depresses the second Ca^{2+} sensor that operates in *syt* I^{AD4}.

Sr^{2+} decreases nerve-evoked synchronous synaptic transmission but enhances asynchronous delayed release and high K^+-induced quantal synaptic events

First, we tested the effect of Sr^{2+} on nerve-evoked release in *P*[*syt* I^{WT}] embryos. In HL3 solution containing 1.0 mM Sr^{2+}, substituting for Ca^{2+}, nerve stimulation evoked synchronous synaptic currents as well as delayed asynchronous events (Fig. 6, *A1* and *A2*). As in HL3 solution containing Ca^{2+}, the synaptic events occurred predominantly between 2 and 10 ms after the onset of the stimulation pulse as shown in the event frequency histogram in Fig. 6*A1* (17 events in the first bin responding to 100 stimuli). The average of the entries in eight bins after stimulation, excluding the first bin, was 5.4 ± 0.7, which was significantly higher than that in five bins before stimulation 1.4 ± 0.5 ($P < 0.01$). We then subtracted the average number of entry of the following eight bins (5.4/bin) from the number of entries in the first bin (17) to estimate the number of events synchronous to nerve stimulation (11.6) as we did for nerve-evoked synaptic events in Ca^{2+}. Thus the quantal content in this cell was 0.12. The average quantal content in six cells was 0.09 ± 0.05, which is significantly smaller than that in HL3 solution containing 1.0 mM Ca^{2+} (1.65 ± 0.47, $n = 8$). However, in the Sr^{2+} solution a few initial stimuli at 0.3 Hz often induced bursts of asynchronous release, which did not subside for many minutes. In those cells we could not measure synchronous release and those data were not used for further analysis. Even in cells in which bursting did not occur, the delayed asynchronous release was prominent (Fig. 6*A1*). The average entry in the eight bins after stimulation, excluding the first bin, was 0.054 ± 0.018 per stimulus,

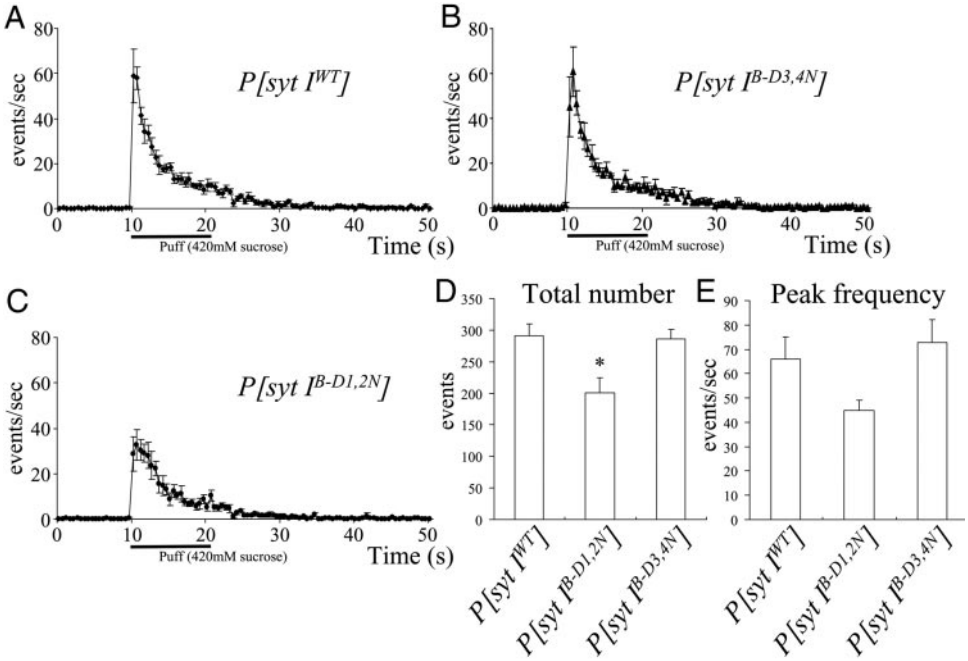

FIG. 5. Hypertonicity responses in a control and two *syt I* transformant embryos. A hypertonic solution (420 mM sucrose was added to the Ca^{2+}-free bath solution) was applied by the puff method with a gas pressure of 0.5 kg/cm^2 for 11 s indicated by the horizontal bar below the abscissa. Bath solution was Ca^{2+}-free saline *A*: *P*[*syt* I^{WT}] ($n = 5$). *B*: *P*[*syt* $I^{B\text{-}D3,4N}$] ($n = 5$). *C*: *P*[*syt* $I^{B\text{-}D1,2N}$] ($n = 6$). *D*: total number of events during each response was counted during a period of 30 s starting at the onset of the puff pulse. Vertical bars attached to each point are the SE. An asterisk indicates a significant difference ($P < 0.05$). *E*: peak frequency (events/s) during the hypertonicity response.

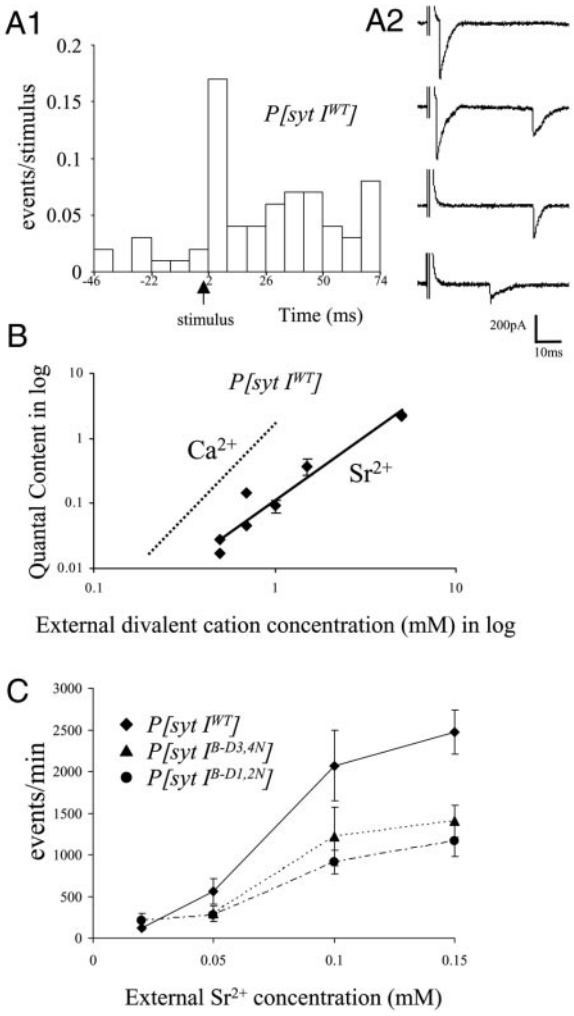

FIG. 6. Synaptic transmission in Sr^{2+}-containing solutions. *A1* and *A2*: a frequency histogram (*A1*) and sample traces (*A2*) of synaptic events evoked by nerve stimulation obtained in a muscle cell of a *P*[*syt* I^{WT}] embryo. Synchronous synaptic events are seen in the first bin after stimulation (during a period between 2 and 10 ms after the onset of stimulus pulse). Asynchronous synaptic events were observed and are depicted in the bins 10 ms or later after stimulation. Total number of stimuli was 102. Sample current traces are shown in *A2*. Recordings were carried out in HL3 medium containing 1.0 mM Sr^{2+} and 20.5 mM Mg^{2+}. Holding potential was −65 mV; stimulus frequency was 0.3 Hz. *B*: relationship between quantal content and external Sr^{2+} concentration in the double-logarithmic plot in *P*[*syt* I^{WT}] embryos. Vertical bars attached to each point are the SE. Straight line was fitted to the all data points (not means) by the least-squares method. Dotted line is for Ca^{2+}, which is reproduced from Fig. 3 for reference. *C*: relationship between the frequency of quantal events induced by high K^+ and the external Sr^{2+} concentration. Quantal events were recorded in an external solution containing 62 mM K^+, 3 μM TTX, and various Sr^{2+} concentrations in embryos of *P*[*syt* I^{WT}] (diamonds), *P*[*syt* $I^{B\text{-}D3,4N}$] (triangles), and *P*[*syt* $I^{B\text{-}D1,2N}$] (circles). Quantal events were counted during a period between 0.5 and 10 min of recording depending on the frequency. Vertical bars attached to each point are the SE. Number of cells for each point was between 4 and 12.

which was significantly higher than the average entry in the five bins preceding stimulus, 0.014 ± 0.011 per stimulus ($P < 0.01$). These properties of synaptic transmission in Sr^{2+} in *P*[*syt* I^{WT}] embryos are similar to those reported in cultured mammalian synapses (Goda and Stevens 1994) and in mouse cerebellar slices (Xu-Friedman and Regehr 2000).

We then examined the external Sr^{2+} concentration dependency of the quantal content in *P*[*syt* I^{WT}] embryos. The slope was 2.01 ± 0.30 ($n = 18$) in the double-logarithmic plot (Fig. 6*B*, diamonds), which was significantly smaller than 2.88 ± 0.43 with Ca^{2+} (diamonds in Fig. 3 and dotted line in Fig. 6*B*, $P < 0.05$). This finding is in accord with the report in mouse cerebellar slices (Xu-Friedman and Regehr 2000).

When Sr^{2+} substitutes for Ca^{2+} in high K^+ solutions, the frequency of quantal events was significantly higher in *P*[*syt* I^{WT}] than that in Ca^{2+}. For example, at 0.1 mM Sr^{2+} the frequency of high K^+-induced quantal events was 2,070 ± 420/min ($n = 8$); this value was much larger than that in 0.1 mM Ca^{2+} (132 ± 34/min, $n = 15$). The frequency of high K^+-induced quantal events increased with the Sr^{2+} concentration (Fig. 6*C*). It was also higher in *P*[*syt* $I^{B\text{-}D3,4N}$] and *P*[*syt* $I^{B\text{-}D1,2N}$] embryos compared with corresponding values in Ca^{2+} and increased with the Sr^{2+} concentration (compare Fig. 4*A* for Ca^{2+} with Fig. 6*C* for Sr^{2+}). The decline of quantal event frequency detected in *P*[*syt* $I^{B\text{-}D1,2N}$] embryos (Fig. 4, *A*, broken line and *B*) was not observed in high K^+ solutions containing Sr^{2+} between 0.02 and 0.15 mM. This observation suggests that Sr^{2+} does not support the negative regulatory function of Syt I.

If the negative regulation of spontaneous vesicle fusion by Syt I is operating in normal saline with Ca^{2+} at the resting state, we expect higher mini frequencies in *P*[*syt* I^{WT}] embryos in Sr^{2+} than in Ca^{2+}. Indeed the mini frequency was 7.3 ± 7.6/min ($n = 10$) in HL3 solution with 1.5 mM Sr^{2+} and 3 μM TTX, which is significantly higher than that in HL3 with 1.5 mM Ca^{2+} and 3 μM TTX (2.6 ± 2.9/min, $n = 15$).

DISCUSSION

We examined the effects of *P*[*syt* $I^{B\text{-}D1,2N}$] and *P*[*syt* $I^{B\text{-}D3,4N}$] mutations expressed in the *syt* I^{null} background on synaptic transmission in embryos. *P*[*syt* $I^{B\text{-}D1,2N}$] virtually abolished synchronous synaptic transmission, whereas *P*[*syt* $I^{B\text{-}D3,4N}$] strongly reduced but did not abolish it. This result indicates that Ca^{2+}-binding sites at the C2B domain are essential for synchronous synaptic transmission. To study the steady-state control on vesicle fusion (negative regulatory function) by Syt I, we examined high K^+-induced quantal release in these mutants and found in *P*[*syt* $I^{B\text{-}D1,2N}$], but not in *P*[*syt* $I^{B\text{-}D3,4N}$], that the frequency of quantal events decreased Ca^{2+} dependently in a narrow range of $[Ca^{2+}]_e$. This finding suggests that the negative regulatory function of Syt I for asynchronous release is Ca^{2+} dependent and preserved in this mutant, although the Ca^{2+} sensing ability for synchronized release by mutated Syt I is profoundly impaired. Sr^{2+} partially substituted Ca^{2+} for synchronous release but did not support the negative regulatory function of Syt I, which specifically requires Ca^{2+}. Thus these two functions of Syt I are distinct.

Each of those mutations is likely to affect both Ca1 and Ca2 binding sites. It is known that the D2N mutation strongly impairs Ca^{2+} binding at both binding sites (Fernandez et al. 2001), which is in accord with our finding that synaptic transmission was more severely depressed in *P*[*syt* $I^{B\text{-}D1,2N}$] than in *P*[*syt* $I^{B\text{-}D3,4N}$] (Fig. 1). Does Ca^{2+} still bind at C2B in these mutants? Because $[Ca^{2+}]_e$ dependency of synchronous synaptic transmission in *P*[*syt* $I^{B\text{-}D3,4N}$] ($n = 1.86 \pm 0.4$) is significantly different from that in *syt* I^{null} (0.95 ± 0.36; Okamoto et al. 2005), it is likely that Ca^{2+} binds to the mutated Syt I in this mutant. Also in *P*[*syt* $I^{B\text{-}D1,2N}$], synchronized

transmitter release was observed in a single cell (Fig. 1*D*). In addition, the frequency of high K^+-induced quantal events at 0.05 mM $[Ca^{2+}]_e$ in *P*[*syt* $I^{B\text{-}D1,2N}$] (53.8 ± 27.3 events/min) was significantly higher than that in *syt* I^{null} (11.7 ± 3.1 events/min; Okamoto et al. 2005). These findings suggest that Ca^{2+} binds to C2B in both transformants.

Nerve-evoked synchronous synaptic transmission in syt I transformants

The effects of these mutations on synaptic transmission were previously studied in third instar larvae (Mackler et al. 2002). In *P*[*syt* $I^{B\text{-}D3,4N}$], nerve-evoked synaptic transmission at NMJs was dramatically depressed compared with that in the control, *P*[*syt* I^{WT}]. Neither immunostaining of nerve terminals with an antibody against Syt I (Mackler et al. 2002) nor the distribution of synaptic vesicles in the presynaptic terminal revealed by electron-microscopic (EM) analysis (Loewen et al. 2006) was different from that in the control. These findings support the idea that the Ca^{2+}-binding sites in C2B are sensing Ca^{2+} for synchronous synaptic transmission. The *P*[*syt* $I^{B\text{-}D1,2N}$] mutation was lethal and not studied in the *syt I*–null background. Instead, synaptic transmission was examined in third instars expressing *P*[*syt* $I^{B\text{-}D1,2N}$] in *syt* I^{WT} heterozygotes. The amplitude of evoked synaptic potentials was strongly depressed to <10% of the control, whereas that in *syt* I^{WT} heterozygotes expressing *P*[*syt* $I^{B\text{-}D3,4N}$] was about 50%. These findings suggest that the mutated Syt I in *P*[*syt* $I^{B\text{-}D1,2N}$] predominantly depresses the function of wild-type Syt I. In *P*[*syt* $I^{B\text{-}D1,2N}$] we found that synchronous synaptic transmission was more severely depressed than that in *syt* I^{null}, *syt* I^{AD4}, whereas the hypertonicity response in the former is much greater than that in the latter (Okamoto et al. 2005). Thus this indicates that the mutated Syt I in *P*[*syt* $I^{B\text{-}D1,2N}$] also suppresses the function of the second Ca^{2+} sensor.

Nishiki and Augustine (2004b) studied the mutations in which each of the aspartates (D) in C2B was individually mutated to asparagines (N) in cultured mouse hippocampal neurons. When mutated Syt I (D2N or D3N) was expressed in *syt I* knockout synapses synchronous synaptic currents were virtually abolished. However, these mutations still suppressed asynchronous release seen in *syt I* knockout synapses. Other substitutions (D1, D4, D5) had relatively minor effects on synaptic transmission. Our results in *P*[*syt* $I^{B\text{-}D1,2N}$] and *P*[*syt* $I^{B\text{-}D3,4N}$] are consistent with theirs, indicating that D2 and D3 are critical for synchronous release.

If Ca1 and Ca2 in C2B are only Ca^{2+}-binding sites in Syt I involved in synchronous synaptic transmission, it is difficult to explain the apparent cooperativity (2.88) in *syt* I^{WT} (Fig. 3), which indicates more than three binding sites are involved for Ca^{2+} detection. This conundrum can be resolved by invoking oligomerization of Syt I.

Ca^{2+}-dependent oligomerization of Syt I

Ca^{2+}-dependent oligomerization occurs at the C2B domain and may be involved in synchronous vesicle fusion (Chapman et al. 1996). A *Drosophila syt I* mutant, *syt* I^{AD3}, has one amino acid substitution in C2B and synchronous synaptic transmission in *syt* I^{AD3} embryos is severely impaired (Okamoto et al. 2005; Yoshihara and Littleton 2002). A homologous mutation in mouse Syt II, which is virtually identical to Syt I (Fernandez et al. 2001), blocks Ca^{2+}-dependent self-oligomerization (Fukuda et al. 2000), and the AD3 mutation impairs Ca^{2+}-dependent oligomerization in *Drosophila* (Littleton et al. 2001). Thus the depressed synaptic transmission in *syt* I^{AD3} may be explained, at least partly, by a defect in Ca^{2+}-dependent oligomerization. Supporting this view, the apparent cooperativity was smaller ($N = 1.54$) in *syt* I^{AD3} compared with 3.01 in a control (Okamoto et al. 2005), which suggests that the binding sites are decreased in this mutant in the absence of oligomerization. However, it is possible that the decreased *N* in *syt* I^{AD3} is the result of other changes induced by this mutation.

Because Sr^{2+} does not induce oligomerization of Syt I (Chapman et al. 1996), we expect synchronous synaptic transmission to be depressed and *N* to be decreased in Sr^{2+}. We found that synchronous synaptic transmission in Sr^{2+} was 5.5% of that in Ca^{2+}, and *N* in Sr^{2+} was 2.01, in contrast to 2.88 in Ca^{2+}. Similarly in mouse cerebellar slices synchronous synaptic transmission in Sr^{2+} is reduced to 7.9% of that in Ca^{2+} and *N* in Sr^{2+} was 1.7, in contrast to 3.2 in Ca^{2+} (Xu-Friedman and Regehr 2000). These data support an involvement of Syt I oligomerization in synchronous transmission. However, a recent crystallographic study showed that the C2B domain binds only one Sr^{2+} (Cheng et al. 2004). The $N = 1.7$ in mice or $N = 2.01$ in *Drosophila* in Sr^{2+} could not be explained with only one binding site without self-oligomerization of Syt I. Alternatively, multiple Syt I molecules without oligomerization might be involved in synchronous release.

In spite of the above arguments that support an involvement of self-oligomerization of Syt I for synchronous release, other reports indicate otherwise. Mackler and Reist (2001) substituted three lysines to glutamines in the C2B domain of Syt I and expressed the mutated Syt I in the *syt I*–null background. This substitution was expected to block Ca^{2+}-dependent oligomerization (Chapman et al. 1998). Nerve-evoked synaptic potentials were depressed by only roughly 36% in the third instar mutant larvae compared with a control. However, this relatively minor effect of the mutation could be a result of developmental compensation for defective synaptic transmission. Borden et al. (2005) recently examined synaptic transmission in cultured mouse neurons that lack endogenous *syt I* but overexpress exogenous mutant *syt I*(Y311N), equivalent to *Drosophila syt* I^{AD3}, or other mutant *syt I*s that are impaired in self-oligomerization. Synaptic transmission was depressed in these synapses, which they explained by a decrease in the Ca^{2+}-binding affinity. They thus concluded that Syt I self-oligomerization plays no role in synaptic transmission. However, to estimate apparent Ca^{2+} dissociation constants they assumed that the maximum response and the cooperativity constant *N* are the same in the mutants as in the control. These assumptions may not be valid because it was previously shown in *syt* I^{AD3} that *N* is significantly smaller (Okamoto et al. 2005).

The frequency of miniature synaptic currents (minis)

The mini frequency is often higher in *syt I*–deficient synapses (DiAntonio and Schwarz 1994; Littleton et al. 1993; Mackler et al. 2002; Pang et al. 2006). In *syt* I^{AD4} embryos, the frequency was similar to that in the control, but because the number of vesicles adjacent to the presynaptic membrane is considerably reduced (Reist et al. 1998) and the hypertonicity

response was roughly 10% of the controls, the release probability of release-ready vesicles must be higher in this mutant compared with that in controls (Okamoto et al. 2005). These findings suggest the negative regulatory function of Syt I on spontaneous release. In this study, we found that the mini frequencies in *P*[*syt I*$^{B\text{-}D1,2N}$] and *P*[*syt I*$^{B\text{-}D3,4N}$] were similar to those in control, and the hypertonicity responses were not greatly different in these mutants. Thus the negative regulatory function of Syt I remains operating in these transformants in spite of severe defects in synchronous release.

High K^+-induced quantal release

The frequency of high K^+-induced synaptic events is lower in *syt I*^{AD3}, compared with that in *syt I*^{AD4}, a *syt I*–null allele (Okamoto et al. 2005), suggesting that Syt I(AD3) inhibits high K^+-induced vesicle fusion. This inhibitory effect was revealed only in *syt I*^{AD3} and not in wild-type, probably because the counteracting enhancing effect of Syt I on vesicle fusion is impaired in this mutant. In *P*[*syt I*$^{B\text{-}D1,2N}$], in which the enhancing effect is further depressed, the frequency of high K^+-induced quantal events was significantly lower at 0.15 mM $[Ca^{2+}]_e$ than at 0.05 mM, suggesting that mutated Syt I in *P*[*syt I*$^{B\text{-}D1,2N}$] Ca^{2+}-dependently inhibits vesicle fusion. The frequency increased again at 0.2 mM Ca^{2+} (Fig. 4*A*), which is probably attributable to facilitatory effects of the mutated Syt I and the second Ca^{2+} sensor. We did not observe this inhibitory effect in *P*[*syt I*$^{B\text{-}D3,4N}$], which probably arises from a stronger remaining facilitatory function of Syt I in this transformant. A Ca^{2+}-dependent decrease of frequency of high K^+-induced quantal synaptic potentials in wild-type animals was previously reported at NMJs (Cooke and Quastel 1973; Ohta and Kuba 1980). Thus the inhibitory effect that we observed in *P*[*syt I*$^{B\text{-}D1,2N}$] is not specific to this mutation. Although we did not observe a similar inhibitory effect in control *Drosophila* embryos, an appropriate combination of K^+ and Ca^{2+} concentrations might reveal such an effect.

The effects of *syt I* mutations on nerve-induced synchronous and asynchronous release and on high K^+-induced quantal release are mediated by the facilitatory functions of Syt I and the second Ca^{2+} sensor as well as by the negative regulatory function of Syt I. Nishiki and Augustine (2004b) observed that D2N and D3N mutations strongly decreased nerve-evoked synchronous release but did not enhance asynchronous release as in *syt I* knockout synapses. In this study we found a clear Ca^{2+}-dependent decrease of the frequency of high K^+-induced quantal events in *P*[*syt I*$^{B\text{-}D1,2N}$], whereas the Ca^{2+} sensing function is greatly reduced. These findings support the idea of dual roles of Syt I (Nishiki and Augustine 2004).

Sr^{2+} does not support the negative regulatory function of Syt I

Nerve-induced synchronous synaptic transmission was strongly depressed but asynchronous release was enhanced in normal Ca^{2+} saline at the NMJ of a *Drosophila syt I*–null mutant (*syt I*^{AD4}; Okamoto et al. 2005; Yoshihara and Littleton 2002) and at synapses formed in culture among neurons derived from *syt I* knockout mice (Geppert et al.,1994; Nishiki and Augustine 2002a,b). The delayed asynchronous release is postulated to be mediated by the high-affinity second Ca^{2+} sensor. It is then possible that wild-type Syt I is negatively regulating the second Ca^{2+} sensor and reducing the delayed release. When Sr^{2+} substitutes for Ca^{2+} synchronous release is reduced, whereas asynchronous release is enhanced. The enhanced asynchronous release in Sr^{2+} is interpreted to be the result of a more efficient activation of the second Ca^{2+} sensor by Sr^{2+} than by Ca^{2+} (Goda and Stevens 1996). Alternatively, in Sr^{2+} solutions Syt I might not effectively regulate asynchronous vesicle fusion. Because we clearly observed a negative regulatory effect of Syt I in *P*[*syt I*$^{B\text{-}D1,2N}$] in high K^+-induced quantal events, we next tested this idea in a solution where Sr^{2+} replaced Ca^{2+}.

We found in control embryos that synchronous synaptic currents in Sr^{2+} were depressed but asynchronous release after nerve stimulation was enhanced. In Sr^{2+} the high K^+-induced synaptic release was more frequent in all strains than in Ca^{2+} and, unlike in Ca^{2+}, was not inhibited concentration dependently in *P*[*syt I*$^{B\text{-}D1,2N}$]. These findings support the idea that Sr^{2+} does not support the negative regulatory function of Syt I, resulting in the enhanced asynchronous release after nerve stimulation as well as higher frequencies of high K^+-induced quantal events and minis in Sr^{2+}. In fact, in *syt I*^{AD4} embryos the high K^+-induced quantal events are not more frequent in Sr^{2+} than in Ca^{2+}, suggesting that Sr^{2+} is not efficient in activating the second Ca^{2+} sensor (Tamura and Kidokoro, unpublished observation). Thus it appears that the negative regulatory function of Syt I is supported by Ca^{2+} but not by Sr^{2+}.

In addition to roles in vesicle fusion Syt I is also implicated for vesicle recycling (Poskanzer et al. 2003; Zhang et al. 1994). Clearly Syt I has multiple functions. Further detailed analyses are required for their elucidation.

ACKNOWLEDGMENTS

Present addresses: T. Tamura, Department of Neuropathology, Medical Research Institute, Tokyo Medical, and Dental University, Bunkyo-ku, Tokyo 113–8510, Japan; J. Hou, University of Florida McKnight Brain Institute, Department of Neuroscience, PO Box 100244, Gainesville, FL 32610–0244; N. E. Reist, Department of Biomedical Sciences, Program in Molecular, Cellular and Integrative Neuroscience, Colorado State University, Fort Collins, CO 80523; and Y. Kidokoro, Department of Physiology, David Geffen School of Medicine at UCLA, 10833 Le Conte Avenue, Los Angeles, CA 90095–1751.

GRANTS

This work was supported by a grant-in-aid for Scientific Research from the Ministry of Education, Culture, Sports, Science and Technology of Japan to Y. Kidokoro and by National Science Foundation Grant (9982962) to N. E. Reist.

REFERENCES

Augustine GJ, Eckert R. Divalent cations differentially support transmitter release at the squid giant synapse. *J Physiol* 346: 257–271, 1984.

Borden CR, Stevens CF, Sullivan JM, Zhu Y. Synaptotagmin mutants Y311N and K326/327A alter the calcium dependence of neurotransmission. *Mol Cell Neurosci* 29: 462–470, 2005.

Broadie K, Bellen H, DiAntonio A, Littleton JT, Schwarz TL. Absence of synaptotagmin disrupts excitation-secretion coupling during synaptic transmission. *Proc Natl Acad Sci USA* 91: 10727–10731, 1994.

Catterall WA. Interactions of presynaptic Ca^{2+} channels and SNARE proteins in neurotransmitter release. *Ann NY Acad Sci* 868: 144–159, 1999.

Chapman ER, An S, Edwardson M, Jahn R. A novel function for the second C2 domain of synaptotagmin. *J Biol Chem* 171: 5844–5849, 1996.

Chapman ER, Desai R, Davis AF, Tornehl CK. Delineation of the oligomerization, AP-2, and synprint-binding region of the C2B-domain of synaptotagmin. *J Biol Chem* 273: 32966–32972, 1998.

Cheng Y, Sequeira SM, Malinina L, Tereshko V, Söllner TH, Patel DJ. Crystallographic identification of Ca^{2+} and Sr^{2+} coordination sites in synaptotagmin I C2B domain. *Protein Sci* 13: 1665–2672, 2004.

Cooke JD, Quastel DMJ. The specific effect of potassium on transmitter release by motor nerve terminals and its inhibition by calcium. *J Physiol* 228: 435–458, 1973.

Deitcher DL, Ueda A, Stewart BA, Burgess RW, Kidokoro Y, Schwarz TL. Distinct requirements for evoked and spontaneous release of neurotransmitter are revealed by mutations in the *Drosophila* gene *neuronal-synaptobrevin. J Neurosci* 18: 2028–2039, 1998.

DiAntonio A, Schwarz TL. The effect on synaptic physiology of synaptotagmin mutations in *Drosophila. Neuron* 12: 909–920, 1994.

Fernandez I, Araç D, Ubach J, Gerber SH, Shin O, Gao Y, Anderson RG, Südhof TC, Rizo J. Three-dimensional structure of the synaptotagmin 1 C_2B-domain: synaptotagmin 1 as a phospholipid binding machine. *Neuron* 32: 1057–1069, 2001.

Fukuda M, Kabayama H, Mikoshiba K. *Drosophila* AD3 mutation of synaptotagmin impairs calcium-dependent self-oligomerization activity. *FASEB Lett* 482: 269–272, 2000.

Geppert M, Goda Y, Hammer RE, Li C, Rosahl TW, Stevens CF, Südhof TC. Synaptotagmin I: a major Ca^{2+} sensor for transmitter release at a central synapse. *Cell* 79: 717–727, 1994.

Goda Y, Stevens CF. Two components of transmitter release at a central synapse. *Proc Natl Acad Sci USA* 91: 12942–12946, 1994.

Hagiwara S, Takahashi K. Surface density of calcium ions and calcium spikes in the barnacle muscle fiber membrane. *J Gen Physiol* 50: 583–561, 1967.

Katz B. *The Release of Neural Transmitter Substances. The Sherrington Lectures X.* Springfield, IL: Charles C. Thomas, 1969.

Kidokoro Y. Roles of SNARE proteins and synaptotagmin I in synaptic transmission: studies at the *Drosophila* neuromuscular synapse. *NeuroSignals* 12: 13–20, 2003.

Kidokoro Y, Nishikawa K. Miniature endplate currents at the newly formed neuromuscular junction in *Drosophila* embryos and larvae. *Neurosci Res* 19: 143–154, 1994.

Koh T-W, Bellen HJ. Synaptotagmin I, a Ca^{2+} sensor for neurotransmitter release. *Trends Neurosci* 26: 413–422, 2003.

Li C, Davletov BA, Südhof TC. Distinct Ca^{2+} and Sr^{2+} binding properties of synaptotagmins. *J Biol Chem* 270: 24898–24902, 1995.

Littleton JT, Bai J, Vyas B, Desai R, Baltus AE, Garment MB, Carlson SD, Ganetzky B, Chapman ER. *synaptotagmin* mutants reveal essential functions for the C2B domain in Ca^{2+}-triggered fusion and recycling of synaptic vesicles *in vivo. J Neurosci* 21: 1421–1433, 2001.

Littleton JT, Ganetzky B. Ion channels and synaptic organization: analysis of the *Drosophila* genome. *Neuron* 26: 35–43, 2000.

Littleton JT, Stern M, Perin M, Bellen HJ. Calcium dependence of neurotransmitter release and rate of spontaneous vesicle fusions are altered in *Drosophila synaptotagmin* mutants. *Proc Natl Acad Sci USA* 91: 10888–10892, 1994.

Loewen CA, Mackler JM, Reist NE. Drosophila synaptotagmin I null mutants survive to early adulthood. *Genesis* 31: 30–36, 2001.

Loewen CA, Rover, SM, Reist NE. Drosophila synaptotagmin I null mutants show severe alterations in vesicle populations, but calcium-binding motif mutants do not. *J Comp Neurol* 496: 1–12, 2006.

Mackler JM, Drummond JA, Loewen CA, Robinson IM, Reist NE. The C2B Ca^{2+}-binding motif of synaptotagmin is required for synaptic transmission *in vivo. Nature* 418: 340–344, 2002.

Mackler JM, Reist NE. Mutations in the second C_2 domain of synaptotagmin disrupt synaptic transmission at *Drosophila* neuromuscular junctions. *J Comp Neurol* 436: 4–16, 2001.

Morimoto T, Popov S, Buckley KM, Poo M-m. Calcium-dependent transmitter secretion from fibroblasts: modulation by synaptotagmin I. *Neuron* 15: 689–696, 1995.

Nishikawa K, Kidokoro Y. Junctional and extrajunctional glutamate receptor channels in *Drosophila* embryos and larvae. *J Neurosci* 15: 7905–7915, 1995.

Nishiki T-I, Augustine GJ. Synaptotagmin I synchronizes transmitter release in mouse hippocampal neurons. *J Neurosci* 24: 6127–6132, 2004a.

Nishiki T-I, Augustine GJ. Dual roles of the C2B domain of synaptotagmin I in synchronizing Ca^{2+}-dependent neurotransmitter release. *J Neurosci* 24: 8542–8550, 2004b.

Ohta Y, Kuba K. Inhibitory action of Ca^{2+} on spontaneous transmitter release at motor nerve terminals in a high K^+ solution. *Pflügers Arch* 386: 29–34, 1980.

Okamoto T, Tamura T, Suzuki K, Kidokoro Y. External Ca^{2+}-dependency of synaptic transmission in *Drosophila synaptotagmin I* mutants. *J Neurophysiol* 94: 1574–1586, 2005.

Pang ZP, Sun J, Rizo J, Maximov A, Südhof TC. Genetic analysis of synaptotagmin 2 in spontaneous and Ca^{2+} triggered neurotransmitter release. *EMBO J* 25: 2039–2050, 2006.

Poskanzer K, Marek KW, Sweeney ST, Davis GW. Synaptotagmin I is necessary for compensatory synaptic vesicle endocytosis *in vivo. Nature* 426: 559–563, 2003.

Reist NE, Buchanan J, Li J, DiAntonio A, Buxton EM, Schwarz TL. Morphologically docked synaptic vesicles are reduced in *synaptotagmin* mutants of *Drosophila. J Neurosci* 18: 7662–7673, 1998.

Robinson IM, Ranjan R, Schwarz TL. Synaptotagmin I and IV promote transmitter release independently of Ca^{2+} binding in the C_2A domain. *Nature* 418: 336–340, 2002.

Rosenmund C, Stevens CF. Definition of the readily releasable pool of vesicles at hippocampal synapses. *Neuron* 16: 1197–1207, 1996.

Stewart BA, Atwood HL, Renger JJ, Wang J, Wu CF. Improved stability of *Drosophila* larval neuromuscular preparations in haemolymph-like physiological solutions. *J Comp Physiol* 175: 179–191, 1994.

Südhof TC, Rizo J. Synaptotagmins: C2-domain proteins that regulate membrane traffic. *Neuron* 17: 379–388, 1996.

Suzuki K, Grinnell AD, Kidokoro Y. Hypertonicity-induced transmitter release at *Drosophila* neuromuscular junctions is partly mediated by integrins and cAMP/PKA. *J Physiol* 538: 103–119, 2002a.

Suzuki K, Okamoto T, Kidokoro Y. Biphasic modulation of synaptic transmission by hypertonicity at the embryonic *Drosophila* neuromuscular junction. *J Physiol* 545: 119–131, 2002b.

Xu-Friedman MA, Regehr WG. Probing fundamental aspects of synaptic transmission with strontium. *J Neurosci* 20: 4414–4422, 2000.

Yoshihara M, Littleton JT. Synaptotagmin I functions as a calcium sensor to synchronize neurotransmitter release. *Neuron* 36: 897–908, 2002.

Zhang D, Kuromi H, Kidokoro Y. Activation of metabotropic glutamate receptors enhances synaptic transmission at the *Drosophila* neuromuscular junction. *Neuropharmacology* 38: 645–657, 1999.

Zhang JZ, Davletov BA, Südhof TC, Anderson RG. Synaptotagmin I is a high affinity receptor for clathrin AP-2: implications for membrane recycling. *Cell* 78: 751–760, 1994.